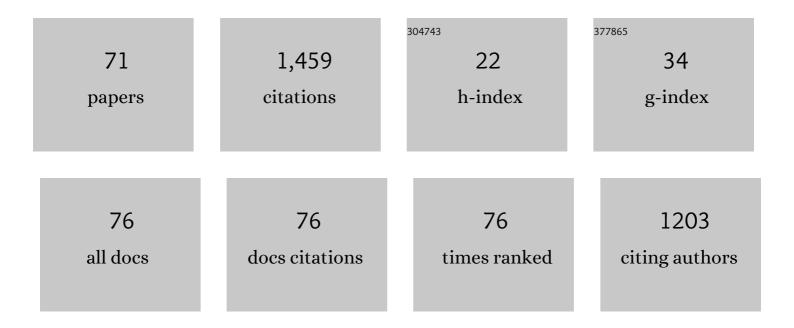
## Lars Nielsen

List of Publications by Year in descending order

Source: https://exaly.com/author-pdf/8150276/publications.pdf Version: 2024-02-01



LADS NIFISEN

#	Article	IF	CITATIONS
1	Rock-physics characterization of chalk by combining acoustic and electromagnetic properties. Geophysics, 2022, 87, MR1-MR11.	2.6	6
2	Optical dating of cobble surfaces determines the chronology of Holocene beach ridges in Greenland. Boreas, 2021, 50, 606-618.	2.4	12
3	Upscaling of outcrop information for improved reservoir modelling – exemplified by a case study on chalk. Petroleum Geoscience, 2021, 27, .	1.5	4
4	Quantitative seismic interpretation of the Lower Cretaceous reservoirs in the Valdemar Field, Danish North Sea. Petroleum Geoscience, 2021, 27, .	1.5	1
5	Practical data acquisition strategy for time-lapse experiments using crosshole GPR and full-waveform inversion. Journal of Applied Geophysics, 2021, 191, 104362.	2.1	4
6	A Holocene relative sea-level database for the Baltic Sea. Quaternary Science Reviews, 2021, 266, 107071.	3.0	29
7	Improved seismic interpretation of a salt diapir by utilization of diffractions, exemplified by 2D reflection seismics, Danish sector of the North Sea. Interpretation, 2020, 8, T77-T88.	1.1	2
8	On the usage of diffractions in ground-penetrating radar reflection data: Implications for time-lapse gas migration monitoring. Geophysics, 2020, 85, H83-H95.	2.6	6
9	Data-driven source wavelets for crosshole ground-penetrating radar full-waveform modeling. , 2020, , .		0
10	Luminescence dating of buried cobble surfaces from sandy beach ridges: a case study from Denmark. Boreas, 2019, 48, 841-855.	2.4	22
11	Deep onshore reflection seismic imaging of the chalk group strata using a 45Âkg accelerated weight-drop and combined recording systems with dense receiver spacing. Geophysics, 2019, 84, B259-B268.	2.6	9
12	Diffraction imaging of ground-penetrating radar data. Geophysics, 2019, 84, H1-H12.	2.6	25
13	MORPHODYNAMICS OF AN ABANDONED DELTA LOBE IN NE GREENLAND. , 2019, , .		0
14	Rock physics templates for chalk by combining acoustic and EM velocity. , 2019, , .		0
15	Pitfalls in velocity analysis for strongly contrasting, layered media – Example from the Chalk Group, North Sea. Journal of Applied Geophysics, 2018, 149, 52-62.	2.1	7
16	Mapping sand layers in clayey till using crosshole ground-penetrating radar. Geophysics, 2018, 83, A21-A26.	2.6	18
17	Sedimentary architecture and depositional controls of a Holocene waveâ€dominated barrierâ€island system. Sedimentology, 2018, 65, 1170-1212.	3.1	22
18	Beach-ridge architecture constrained by beach topography and ground-penetrating radar, Itilleq (Laksebugt), south-west Disko, Greenland – implications for sea-level reconstructions Bulletin of the Geological Society of Denmark, 2018, 66, 167-179.	1.1	3

Lars Nielsen

#	Article	IF	CITATIONS
19	Full-waveform inversion of Crosshole GPR data: Implications for porosity estimation in chalk. Journal of Applied Geophysics, 2017, 140, 102-116.	2.1	34
20	Sea-level proxies in Holocene raised beach ridge deposits (Greenland) revealed by ground-penetrating radar. Scientific Reports, 2017, 7, 46460.	3.3	20
21	High-resolution shear-wave seismics across the Carlsberg Fault zone south of Copenhagen — Implications for linking Mesozoic and late Pleistocene structures. Tectonophysics, 2016, 682, 56-64.	2.2	12
22	Early diagenetic evolution of Chalk in eastern Denmark. Depositional Record, 2016, 2, 154-172.	1.7	9
23	Coastal lagoons and beach ridges as complementary sedimentary archives for the reconstruction of Holocene relative seaâ€evel changes. Terra Nova, 2016, 28, 43-49.	2.1	25
24	Continuous record of Holocene sea-level changes and coastal development of the Kattegat island LæsÃ, (4900 years BP to present). Bulletin of the Geological Society of Denmark, 2016, 64, 1-55.	1.1	12
25	Estimation of Recharge from Longâ€Term Monitoring of Saline Tracer Transport Using Electrical Resistivity Tomography. Vadose Zone Journal, 2015, 14, 1-13.	2.2	14
26	Changes in Holocene relative sea-level and coastal morphology: A study of a raised beach ridge system on SamsÃ, southwest Scandinavia. Holocene, 2015, 25, 1402-1414.	1.7	30
27	Stratigraphy, Evolution, and Controls of A Holocene Transgressive–Regressive Barrier Island Under Changing Sea Level: Danish North Sea Coast. Journal of Sedimentary Research, 2015, 85, 820-844.	1.6	47
28	Simultaneous estimation of lithospheric uplift rates and absolute sea level change in southwest Scandinavia from inversion of sea level data. Geophysical Journal International, 2014, 199, 1018-1029.	2.4	6
29	Morphological records of storm floods exemplified by the impact of the 1872 Baltic storm on a sandy spit system in southâ€eastern Denmark. Earth Surface Processes and Landforms, 2014, 39, 499-508.	2.5	20
30	Full-waveform inversion of cross-hole GPR data collected in a strongly heterogeneous chalk reservoir analogue with sharp permittivity and conductivity contrasts. , 2014, , .		0
31	Examining the information content of time-lapse crosshole GPR data collected under different infiltration conditions to estimate unsaturated soil hydraulic properties. Advances in Water Resources, 2013, 54, 38-56.	3.8	10
32	Joint interpretation of beach-ridge architecture and coastal topography show the validity of sea-level markers observed in ground-penetrating radar data. Holocene, 2013, 23, 1238-1246.	1.7	33
33	GENERATING RADAR-WAVE VELOCITY FIELD FOR DEPTH CONVERSION USING INFORMATION ON GROUNDWATER LEVEL. , 2013, , .		2
34	Bayesian Markovâ€Chainâ€Monteâ€Carlo Inversion of Timeâ€Lapse Crosshole GPR Data to Characterize the Vadose Zone at the Arrenaes Site, Denmark. Vadose Zone Journal, 2012, 11, vzj2011.0153.	2.2	21
35	Quantitative constraints on the sea-level fall that terminated the Littorina Sea Stage, southern Scandinavia. Quaternary Science Reviews, 2012, 40, 54-63.	3.0	30
36	Morphology and sedimentary architecture of a beachâ€ridge system ( <scp>A</scp> nholt, the) Tj ETQq0 0 0 rgBT	/Overlock 2.4	10 Tf 50 67 25

past â^1⁄41000 years. Boreas, 2012, 41, 422-434.

LARS NIELSEN

#	Article	IF	CITATIONS
37	Comparing Plume Characteristics Inferred from Crossâ€Borehole Geophysical Data. Vadose Zone Journal, 2012, 11, vzj2012.0031.	2.2	14
38	Visualizing Unsaturated Flow Phenomena Using Highâ€Resolution Reflection Ground Penetrating Radar. Vadose Zone Journal, 2011, 10, 84-97.	2.2	45
39	Integrated seismic analysis of the Chalk Group in eastern Denmark—Implications for estimates of maximum palaeo-burial in southwest Scandinavia. Tectonophysics, 2011, 511, 14-26.	2.2	20
40	Coastal evolution of a cuspate foreland (Flakket, Anholt, Denmark) between 2006 and 2010 Bulletin of the Geological Society of Denmark, 2011, 59, 37-44.	1.1	8
41	Internal architecture of a raised beach ridge system (Anholt, Denmark) resolved by ground-penetrating radar investigations. Sedimentary Geology, 2010, 223, 281-290.	2.1	68
42	23. Estimation of Chalk Heterogeneity from Stochastic Modeling Conditioned by Crosshole GPR Traveltimes and Log Data. , 2010, , 379-396.		13
43	Geostatistical inference using crosshole ground-penetrating radar. Geophysics, 2010, 75, J29-J41.	2.6	17
44	Threeâ€dimensional architecture and development of Danian bryozoan mounds at Limhamn, southâ€west Sweden, using groundâ€penetrating radar. Sedimentology, 2009, 56, 695-708.	3.1	9
45	Seaâ€level markers identified in groundâ€penetrating radar data collected across a modern beach ridge system in a microtidal regime. Terra Nova, 2009, 21, 474-479.	2.1	40
46	Quantifying the influence of static-like errors in least-squares-based inversion and sequential simulation of cross-borehole ground penetrating radar data. Journal of Applied Geophysics, 2009, 68, 71-84.	2.1	24
47	Integrating ground-penetrating radar and borehole data from a Wadden Sea barrier island. Journal of Applied Geophysics, 2009, 68, 47-59.	2.1	24
48	Layered crust–mantle transition zone below a large crustal intrusion in the Norwegian–Danish Basin. Tectonophysics, 2009, 472, 194-212.	2.2	13
49	Monitoring Unsaturated Flow and Transport Using Crossâ€Borehole Geophysical Methods. Vadose Zone Journal, 2008, 7, 227-237.	2.2	112
50	Inferring the Subsurface Structural Covariance Model Using Crossâ€Borehole Ground Penetrating Radar Tomography. Vadose Zone Journal, 2008, 7, 249-262.	2.2	20
51	ldentifying Unsaturated Hydraulic Parameters Using an Integrated Data Fusion Approach on Crossâ€Borehole Geophysical Data. Vadose Zone Journal, 2008, 7, 238-248.	2.2	96
52	Accounting for Correlated Data Errors during Inversion of Crossâ€Borehole Ground Penetrating Radar Data. Vadose Zone Journal, 2008, 7, 263-271.	2.2	22
53	Mapping of the freshwater lens in a coastal aquifer on the Keta Barrier (Ghana) by transient electromagnetic soundings. Journal of Applied Geophysics, 2007, 62, 1-15.	2.1	24
54	ldentification of crustal and upper mantle heterogeneity by modelling of controlled-source seismic data. Tectonophysics, 2006, 416, 209-228.	2.2	22

LARS NIELSEN

#	Article	IF	CITATIONS
55	Seismic velocity structure of a large mafic intrusion in the crust of central Denmark from project ESTRID. Tectonophysics, 2006, 420, 105-122.	2.2	19
56	Seismic tomographic interpretation of Paleozoic sedimentary sequences in the southeastern North Sea. Geophysics, 2005, 70, R45-R56.	2.6	11
57	Integrated seismic interpretation of the Carlsberg Fault zone, Copenhagen, Denmark. Geophysical Journal International, 2005, 162, 461-478.	2.4	8
58	Ground-penetrating radar imaging of carbonate mound structures and implications for interpretation of marine seismic data. AAPG Bulletin, 2004, 88, 1069-1082.	1.5	15
59	Location of the Carlsberg Fault zone from seismic controlled-source fan recordings. Geophysical Research Letters, 2004, 31, n/a-n/a.	4.0	9
60	TeleseismicPnarrivals: influence of mantle velocity gradient and crustal scattering. Geophysical Journal International, 2003, 152, F1-F7.	2.4	16
61	Origin of upper-mantle seismic scattering - evidence from Russian peaceful nuclear explosion data. Geophysical Journal International, 2003, 154, 196-204.	2.4	33
62	The origin of teleseismicPnwaves: Multiple crustal scattering of upper mantle whispering gallery phases. Journal of Geophysical Research, 2003, 108, .	3.3	29
63	Seismic scattering at the top of the mantle Transition Zone. Earth and Planetary Science Letters, 2003, 216, 259-269.	4.4	24
64	Implications of seismic scattering below the 8° discontinuity along PNE profile Kraton. Tectonophysics, 2002, 358, 135-150.	2.2	35
65	Constraints on reflective bodies below the 8° discontinuity from reflectivity modelling. Geophysical Journal International, 2001, 145, 759-770.	2.4	15
66	Integrated gravity and wide-angle seismic inversion fortwo-dimensional crustal modelling. Geophysical Journal International, 2000, 140, 222-232.	2.4	46
67	Seismic and gravity modelling of crustal structure in the Central Graben, North Sea. Observations along MONA LISA profile 3. Tectonophysics, 2000, 328, 229-244.	2.2	31
68	Seismic tomographic inversion of Russian PNE data along profile Kraton. Geophysical Research Letters, 1999, 26, 3413-3416.	4.0	42
69	Seismic evidence for deep Palaeozoic sedimentary units in the RingkÃ,bing-Fyn High offshore Denmark. Bulletin of the Geological Society of Denmark, 1998, 45, 1-10.	1.1	9
70	Geophysics for urban mining and the first surveys in Denmark: rationale, field activity and preliminary results. Geological Survey of Denmark and Greenland Bulletin, 0, , .	2.0	2
71	Seismic interpretation pitfalls caused by interference effects, exemplified by seismic modeling of outcropping chalk successions. Interpretation, 0, , 1-31.	1.1	1